Spectral Based Discontinuous Galerkin Reduced Basis Element Method for Parametrized Stokes Problems[1]

Paolo Pacciarini[a], Paola Gervasio[b], Alfio Quarteroni[c]

[a] *MOX–Modeling and Scientific Computing, Dipartimento di Matematica, Politecnico di Milano, Piazza Leonardo da Vinci 32, 20133 Milano, Italy*
[b] *DICATAM, Università degli Studi di Brescia, via Branze 38, Brescia, Italy*
[c] *CMCS-MATHICSE, École Polytechnique Fédérale de Lausanne (EPFL), Station 8, 1015 Lausanne, Switzerland*[2]

Abstract

In this work we extend to the Stokes problem the Discontinuous Galerkin Reduced Basis Element (DGRBE) method introduced in [1]. By this method we aim at reducing the computational cost for the approximation of a parametrized Stokes problem on a domain partitioned into subdomains. During an *offline* stage, expensive but performed only once, a low-dimensional approximation space is built on each subdomain. For any new value of the parameter, the rapid evaluation of the solution takes place during the *online* stage and consists in a Galerkin projection onto the low-dimensional subspaces computed offline. The *high-fidelity* discretization on each subdomain, used to build the local low-dimensional subspaces, is based on spectral element methods. The continuity of both the velocity and the normal component of the Cauchy stress tensor at subdomain interfaces is weakly enforced by a discontinuous Galerkin approach.

Keywords: Reduced Basis Element method; Discontinuous Galerkin; Domain decomposition; Spectral element methods; Parametrized PDE; Stokes equations

1. Introduction

The numerical approximation of Parametrized Partial Differential Equations (PPDEs) is a challenging task, especially when a rapid computation of the solution is required for a new given value of the parameter. In many applications, for instance real-time simulations, resorting to approximation methods like the Finite Element Method (FEM) or the Spectral Element Method (SEM) can be too computationally demanding. To face this problem, a wide range of model order reduction techniques have been proposed. The Reduced Basis (RB) method have been successfully developed for problems defined on a single parametrized domain, see [2] for a comprehensive presentation. The RB method provides an approximate solution of the PPDE using a small number of basis functions, computed by a *high-fidelity* discretization of the given PPDE consisting of a Galerkin method like FEM or SEM, typically featuring a very large number of degrees of freedom. In case of partitioned domains, a suitable variant of the RB method is the so-called Reduced Basis Element (RBE) method. This approach has been introduced in [3, 4] for elliptic problems and then extended to the Stokes problem in [5, 6]. Its main feature is that local bases are built on every subdomain with the aim that the space spanned by such local bases is able to represent the global reduced solution computed through a Galerkin projection. Thus, in the RBE context, a major issue is to enforce the continuity of the global reduced solution as well as the continuity of its flux (or of the normal component of the Cauchy stress

[1] Accepted for publication on Computers and Mathematics with Applications (2016), doi:10.1016/j.camwa.2016.01.030
[2] On leave at MOX–Modeling and Scientific Computing, Dipartimento di Matematica, Politecnico di Milano, Piazza Leonardo da Vinci 32, 20133 Milano, Italy
Email addresses: paolo.pacciarini@gmail.com (Paolo Pacciarini), paola.gervasio@unibs.it (Paola Gervasio), alfio.quarteroni@epfl.ch (Alfio Quarteroni)

tensor), by preserving the locality of the method and preventing it to become computationally unbearable. Several approaches have been adopted to address this purpose until now, the most used are those based on the introduction of Lagrange multipliers [7] and the discontinuous Galerkin (DG) method [8].

In the last years several improvements of the original idea of RBE have been proposed. We recall for instance the static condensation Reduced Basis Element Method [9, 10, 11], based on the approximation of the Schur complement that depends solely on the interface variables, and the Reduced Basis Hybrid Method [12], developed in particular for the Stokes problem. In the latter, the continuity of the velocity is enforced by using Lagrange multiplier at the interfaces while in order to recover the continuity of the normal component of the Cauchy stress tensor a global coarse mesh is overlaid to the local bases. The issue of the continuity can also be faced by introducing additional degrees of freedom corresponding to the high-fidelity FEM basis functions on the interface, as it is done in the Reduced basis – Domain decomposition – Finite elements (RDF) method [13]. Other approaches, similar to the RBE method, are also used for coupled problems [14] as well as in the RB–multiscale research branch [15, 16].

In the present work we focus on the Discontinuous Galerkin Reduced Basis Element method (DGRBE). This method, originally proposed in [1] for elliptic problems, relies on a discontinuous global reduced space that is spanned by local bases built independently on each subdomain, that satisfy non-homogeneous Neumann conditions on the interface in order to enhance the accuracy of the method. The (weak) continuity of the solution and of the fluxes across the interfaces is recovered through a DG approach.

In this paper, we extend the DGRBE method to the Stokes problem. In such a case, the DG approach aims to recover the (weak) continuity of the velocity and that of the normal component of the Cauchy stress tensor at the interfaces. The main issue to address here is the stability of the reduced problem. Indeed, differently from the elliptic case, the well-posedness of the global Stokes reduced problem is not necessarily inherited from that of the global high-fidelity problem. More specifically, the condition that can get lost at the reduced level is the inf-sup compatibility between the velocity and the pressure spaces. In order to overcome such a drawback we adopt a technique proposed in [17] in the single domain case to enrich the velocities of the snapshot system built during the Greedy step. Another novelty with respect to [1] is that here a SEM (rather than a FEM) high-fidelity discretization is used. The reason is that SEM is more coherent with the interface enrichment that is made of high order Legendre polynomials. In our numerical tests we investigate the relation between the accuracy of the reduced model and the order of the Legendre polynomials considered for the interface enrichment and we show that the DGRBE method can be convenient in terms of computational savings.

This work is structured as follows: in Section 2 we introduce the model problem and give the main definitions, in Section 3 we introduce the high-fidelity model and discuss its well posedness, in Section 4 we present and analyse the DGRBE method for Stokes problem and, finally, in Section 5 we show some numerical results in order to assess the performance of the method.

2. Model problem

Let Ω be a bounded open subset of $\mathbb{R}^2$ such that $\overline{\Omega} = \bigcup_{i=1}^{N_S} \overline{\Omega}_i$, where $\Omega_i \subset \mathbb{R}^2$, $i = 1, \dots, N_S$. We also assume that the partition is non-overlapping, *i.e.*, $\Omega_i \cap \Omega_j = \emptyset$ when $i \neq j$. Let then $\mathcal{D} \subset \mathbb{R}^P$ be the parameter space. We consider the following Stokes equation: given $\boldsymbol{\mu} \in \mathcal{D}$, find $(\boldsymbol{u}(\boldsymbol{\mu}), p(\boldsymbol{\mu})) \in [H^1(\Omega)]^2 \times L^2(\Omega)$ such that

$$
\begin{aligned}
-\operatorname{div}(\nu(\boldsymbol{\mu})\nabla \boldsymbol{u}(\boldsymbol{\mu})) + \nabla p(\boldsymbol{\mu}) &= \boldsymbol{f}(\boldsymbol{\mu}) \quad && \text{in } \Omega \\
\operatorname{div} \boldsymbol{u}(\boldsymbol{\mu}) &= 0 && \text{in } \Omega \\
\boldsymbol{u} &= \boldsymbol{g}(\boldsymbol{\mu}) && \text{on } \Sigma_D \subseteq \partial\Omega \\
\nu(\boldsymbol{\mu})\frac{\partial \boldsymbol{u}(\boldsymbol{\mu})}{\partial \boldsymbol{n}} - p(\boldsymbol{\mu})\boldsymbol{n} &= \boldsymbol{h}(\boldsymbol{\mu}) && \text{on } \Sigma_N = \partial\Omega \backslash \Sigma_D
\end{aligned}
\tag{1}
$$

where $\boldsymbol{n}$ is the outward pointing normal unit vector to $\partial\Omega$, $\nu(\boldsymbol{\mu})$ is the viscosity, $\boldsymbol{f}(\boldsymbol{\mu}) \in [L^2(\Omega)]^2$ is a forcing term, while $\boldsymbol{g}(\boldsymbol{\mu}) \in H^{1/2}(\Sigma_D)$ and $\boldsymbol{h}(\boldsymbol{\mu}) \in H^{-1/2}(\Sigma_N)$ are given data on the boundaries Σ_D and Σ_N respectively, where $\Sigma_D \cup \Sigma_N = \partial\Omega$ and $\Sigma_D \cap \Sigma_N = \emptyset$. We require that $\partial\Omega_i \cap \Sigma_D \neq \emptyset$ for $i = 1, \dots, N_S$. We denote with Γ_{ij} the interface between the subdomains Ω_i and Ω_j and we define $\Gamma = \bigcup_{i,j=1}^{N_S} \Gamma_{ij}$. We

assume that $\nu(\boldsymbol{\mu})$ is constant over the global domain Ω, in particular we set $\nu(\boldsymbol{\mu}) = \mu_0$ with $\mu_0 \in \mathcal{D}_0 \subset \mathbb{R}^+$. We assume that $\mathcal{D} \subset \prod_{i=0}^{N_S} \mathcal{D}_i$, where $\mathcal{D}_i$, for $i = 1, \ldots, N_S$, is a subset of $\mathbb{R}^{P_i}$. We denote with $\boldsymbol{\mu} = (\mu_0, \boldsymbol{\mu}_1, \ldots, \boldsymbol{\mu}_{N_S})$ a generic element of $\mathcal{D}$, where $\boldsymbol{\mu}_i \in \mathcal{D}_i$, for $i = 1, \ldots, N_S$. Of course we require that $P = 1 + \sum_{i=1}^{N_S} P_i$. We finally assume that the forcing term and the boundary data, restricted to Ω_i depend only on $\boldsymbol{\mu}_i$, that is

$$\boldsymbol{f}(\boldsymbol{\mu})|_{\Omega_i} = \boldsymbol{f}_i(\boldsymbol{\mu}_i), \quad \boldsymbol{g}(\boldsymbol{\mu})|_{\Omega_i} = \boldsymbol{g}_i(\boldsymbol{\mu}_i), \quad \boldsymbol{h}(\boldsymbol{\mu})|_{\Omega_i} = \boldsymbol{h}_i(\boldsymbol{\mu}_i).$$

The viscosity ν is taken independent of the parameters $\boldsymbol{\mu}_1, \ldots, \boldsymbol{\mu}_{N_s}$ since we are assuming that the fluid is the same in the whole domain Ω. Nevertheless, our method can be extended to equations of different nature like, e.g., the bi-harmonic one, in which the coefficient of the second order derivatives (the analogous of ν) is related to Young's modulus of the elastic material. The method is still well-posed even if such coefficient is piece-wise constant (subdomain by subdomain) and it depends on the parameters $\boldsymbol{\mu}_1, \ldots, \boldsymbol{\mu}_{N_s}$.

Remark 1. To ease the presentation of our method we considered only "physical" parameters, *i.e.*, parameters affecting only the coefficients and the right-hand side of the equation (for instance the viscosity, the inlet velocity), and not "geometrical" parameters that characterize the domain itself, *cf.* [18, 2]. When the domain is parameter-dependent, it is customary to trace the problem back onto a parameter-independent domain. In that case, on the reference domain, the geometrical parameters affect (through the transformation mapping) the problem coefficients, and behave as if they were physical ones. In this context, in particular we deal with anisotropic viscosity tensors $\nu(\boldsymbol{\mu})$ that are discontinuous along the interfaces of the reference domain and depend on the local geometrical parameters. However, our approach allows to effectively handle these situations.

3. High-fidelity approximation

We introduce now the high-fidelity model, which we aim to reproduce using our reduced order approximation that will be presented in Section 4. First of all, on each subdomain Ω_i we define a conforming quadrilateral mesh $\mathcal{T}_{h,i}$. Here h denotes the maximum element edge length. More precisely, we assume that each element K of $\mathcal{T}_{h,i}$ is the image through an invertible and differentiable map T_K, with differentiable inverse, of the reference square $\widehat{K} = [-1, 1]^2$. We also assume that $\|\boldsymbol{v}\|_{H^1(K)} \sim ch_K^{-1}\|\hat{\boldsymbol{v}}\|_{H^1(\widehat{K})}$ if $\boldsymbol{v} \in H^1(K)$ and $\widehat{\boldsymbol{v}} \in H^1(\widehat{K})$ are related by the Piola transform (this is true, *e.g.*, if T_K is either affine or quadratic), see [19]. We finally require that each $\mathcal{T}_{h,i}$ satisfies the usual hypotheses of shape regularity and quasi-uniformity. We denote with $\mathbb{Q}_p(\widehat{K})$ the space of the polynomials defined on $\widehat{K}$, of degree at most p in each variable. We then introduce the space

$$\mathbb{Q}_p(\mathcal{T}_{h,i}) = \{z \in L^2(\Omega_i) \mid z|_K \circ T_K \in \mathbb{Q}_p(\widehat{K}) \quad \forall\, K \in \mathcal{T}_{h,i}\}.$$

We then define the local approximation spaces, for $i = 1, \ldots, N_S$,

$$V_i^{\mathcal{N}} = \{\boldsymbol{v} \in [L^2(\Omega)]^2 \mid \boldsymbol{v}|_{\Omega_i} \in [\mathbb{Q}_p(\mathcal{T}_{h,i}) \cap C^0(\overline{\Omega}_i)]^2, \boldsymbol{v} = \boldsymbol{0} \text{ in } \Omega \backslash \Omega_i\},$$
$$Q_i^{\mathcal{N}} = \{q \in L^2(\Omega) \mid q|_{\Omega_i} \in \mathbb{Q}_{p-2}(\mathcal{T}_{h,i}), q = 0 \text{ in } \Omega \backslash \Omega_i\}$$

with $p \geq 2$, and the global ones (the symbol $\bigoplus$ means direct sum):

$$V^{\mathcal{N}} = \bigoplus_{i=1}^{N_S} V_i^{\mathcal{N}}, \quad Q^{\mathcal{N}} = \bigoplus_{i=1}^{N_S} Q_i^{\mathcal{N}}.$$

Here $\mathcal{N}$ generically refers to the dimension of the high-fidelity space. More precisely we denote with $\mathcal{N}_i^V$, $\mathcal{N}^V$, $\mathcal{N}_i^Q$, $\mathcal{N}^Q$ the dimensions of $V_i^{\mathcal{N}}$, $V^{\mathcal{N}}$, $Q_i^{\mathcal{N}}$, $Q^{\mathcal{N}}$ respectively. In this setting, we can express each element $\boldsymbol{v}^{\mathcal{N}} \in V^{\mathcal{N}}$ and $q^{\mathcal{N}} \in Q^{\mathcal{N}}$ as

$$\boldsymbol{v}^{\mathcal{N}} = \sum_{i=1}^{N_S} \boldsymbol{v}_i^{\mathcal{N}}, \quad q^{\mathcal{N}} = \sum_{i=1}^{N_S} q_i^{\mathcal{N}}, \quad \text{with} \quad \boldsymbol{v}_i^{\mathcal{N}} \in V_i^{\mathcal{N}}, \quad q_i^{\mathcal{N}} \in Q_i^{\mathcal{N}} \quad \text{for} \quad i = 1, \ldots, N_S.$$

and these representations are unique. We look for two Lagrangian interpolation bases: that of $V_i^{\mathcal{N}}$ is associated with the Gauss-Legendre-Lobatto (GLL) nodes ($(p+1)^2$ in $\overline{K}$), while the one of $Q_i^{\mathcal{N}}$ with the Gauss-Legendre (GL) nodes ($(p-1)^2$ in $\overline{K}$), *cf.* [20, 19] for the definition and further details. The elements of the global spaces $V^{\mathcal{N}}$ are continuous inside each subdomain Ω_i but discontinuous along the interfaces Γ_{ij}. The idea underlying our method is to use a spectral element method with numerical integration based on Gauss-Lobatto formulae inside each subdomain, *i.e.*, a SEM-NI approach [19], while exploiting DG techniques in order to recover the (weak) continuity of the velocities and that of the Cauchy normal stresses along the interfaces [21, 22, 23, 24].

Having that in mind, for $i = 1, \ldots, N_S$, for each $K \in \mathcal{T}_{h,i}$ we introduce the following inner product

$$(w_K, v_K)_K = \sum_{k,l=1}^{p+1} [w_K \circ T_K(\xi_k, \xi_l)]\, [v_K \circ T_K(\xi_k, \xi_l)]\, \omega_k \omega_l \, |\det JT_K| \quad \forall\, w_K, v_K \in C^0(\overline{K}),$$

where ξ_q, $q = 1, \ldots, p+1$ are the GLL quadrature nodes on $[-1, 1]$ and ω_q the associated integration weights. We have denoted with JT_K the Jacobian matrix of the transformation T_K. We can now define the discrete subdomain-level products

$$(w, v)_{\Omega_i} = \sum_{K \in \mathcal{T}_{h,i}} (w|_K, v|_K)_K \quad \forall\, w, v \in C^0(\mathcal{T}_{h,i}).$$

where

$$C^0(\mathcal{T}_{h,i}) = \{z \in L^2(\Omega_i) \mid z|_K \in C^0(\overline{K}) \quad \forall\, K \in \mathcal{T}_{h,i}\}.$$

To keep the presentation simple, in this work we assume that the local meshes $\mathcal{T}_{h,i}$ are conforming at the interfaces, *i.e.*, $\mathcal{T}_h = \bigcup_{i=1}^{N_S} \mathcal{T}_{h,i}$ is a global conforming quadrilateral mesh. However, the DG approach can be effectively combined with the SEM even in case of non-conforming grids, as shown in [25]. Then each interface Γ_{ij} is the union of straight segments e that are edges of elements of $\mathcal{T}_{h,i}$ (or, equivalently, $\mathcal{T}_{h,j}$). Clearly, also the boundary regions $\partial\Omega_i \cap \partial\Omega$ can be seen as union of segments e such that both $\partial\Omega \cap \Sigma_D$ and $\partial\Omega \cap \Sigma_N$ do not cut any e. Denoting with T_e the affine transformation that maps $\widehat{e} = [-1, 1]$ onto e, we define

$$(w_e, v_e)_e = \sum_{k=1}^{p+1} [w_e \circ T_e(\xi_k)][v_e \circ T_e(\xi_k)]\, \omega_k \, |T_e'| \quad \forall\, w_e, v_e \in C^0(\overline{e}).$$

We define the following sets

$$\mathcal{E}_{ij} = \{e \mid e \subset \Gamma_{ij}\}, \quad \mathcal{E}_{i,D} = \{e \mid e \subset \partial\Omega_i \cap \Sigma_D\}, \quad \mathcal{E}_{i,N} = \{e \mid e \subset \partial\Omega_i \cap \Sigma_N\}$$

and introduce the scalar products

$$\begin{aligned}
(w, v)_{\Gamma_{ij}} &= \sum_{e \in \mathcal{E}_{ij}} (w|_e, v|_e)_e\,, \quad && \forall\, w, v \in C^0(\overline{\Gamma}_{ij}) \\
(w, v)_{\partial\Omega_i \cap \Sigma_D} &= \sum_{e \in \mathcal{E}_{i,D}} (w|_e, v|_e)_e\,, && \forall\, w, v \in C^0(\overline{\Sigma}_{D,i}) \\
(w, v)_{\partial\Omega_i \cap \Sigma_N} &= \sum_{e \in \mathcal{E}_{i,N}} (w|_e, v|_e)_e && \forall\, w, v \in C^0(\overline{\Sigma}_{N,i}).
\end{aligned}$$

We introduce the local forms

$$\begin{aligned}
A_i(\boldsymbol{w}_i^{\mathcal{N}}, \boldsymbol{v}_i^{\mathcal{N}}; \mu_0) &= \mu_0 \left(\nabla \boldsymbol{w}_i^{\mathcal{N}}, \nabla \boldsymbol{v}_i^{\mathcal{N}}\right)_{\Omega_i} - \mu_0 \left(\nabla \boldsymbol{w}_i^{\mathcal{N}}\, \boldsymbol{n}_i, \boldsymbol{v}_i^{\mathcal{N}}\right)_{\partial\Omega_i \cap \Sigma_D} - \mu_0 \left(\nabla \boldsymbol{v}_i^{\mathcal{N}}\, \boldsymbol{n}_i, \boldsymbol{w}_i^{\mathcal{N}}\right)_{\partial\Omega_i \cap \Sigma_D} \\
&\quad + \gamma\, \mu_0 \frac{p^2}{h} \left(\boldsymbol{w}_i^{\mathcal{N}}, \boldsymbol{v}_i^{\mathcal{N}}\right)_{\partial\Omega_i \cap \Sigma_D}, \\
B_i(\boldsymbol{v}_i^{\mathcal{N}}, q_i^{\mathcal{N}}) &= -\left(q_i^{\mathcal{N}}, \operatorname{div} \boldsymbol{v}_i^{\mathcal{N}}\right)_{\Omega_i} + \left(q_i^{\mathcal{N}}, \boldsymbol{v}_i^{\mathcal{N}} \cdot \boldsymbol{n}_i\right)_{\partial\Omega_i \cap \Sigma_D}, \\
F_i(\boldsymbol{v}_i^{\mathcal{N}}; \mu_0, \boldsymbol{\mu}_i) &= \left(\boldsymbol{f}_i(\boldsymbol{\mu}_i), \boldsymbol{v}_i^{\mathcal{N}}\right)_{\Omega_i} - \mu_0 \left(\boldsymbol{g}_i(\boldsymbol{\mu}_i), \nabla \boldsymbol{v}_i^{\mathcal{N}}\, \boldsymbol{n}_i\right)_{\partial\Omega_i \cap \Sigma_D} + \gamma\, \mu_0 \frac{p^2}{h} \left(\boldsymbol{g}_i(\boldsymbol{\mu}_i), \boldsymbol{v}_i^{\mathcal{N}}\right)_{\partial\Omega_i \cap \Sigma_D} \\
&\quad + \left(\boldsymbol{h}_i(\boldsymbol{\mu}_i), \boldsymbol{v}_i^{\mathcal{N}}\right)_{\partial\Omega_i \cap \Sigma_N}, \\
G_i(q_i^{\mathcal{N}}; \boldsymbol{\mu}_i) &= \left(q_i^{\mathcal{N}}, \boldsymbol{g}_i(\boldsymbol{\mu}_i) \cdot \boldsymbol{n}_i\right)_{\partial\Omega_i \cap \Sigma_D}
\end{aligned}$$

for each $\boldsymbol{w}_i^{\mathcal{N}}$, $\boldsymbol{v}_i^{\mathcal{N}} \in V_i^{\mathcal{N}}$ and for each $q_i^{\mathcal{N}} \in Q_i^{\mathcal{N}}$, where $\boldsymbol{n}_i$ is the outward pointing unit vector normal to $\partial\Omega_i$. The coefficient $\gamma > 0$ has a stabilization role that will be discussed in the following. The products between non-scalar quantities have to be intended component-wise. We then define the global bilinear forms

$$\begin{aligned}
A_{DG}(\boldsymbol{w}^{\mathcal{N}}, \boldsymbol{v}^{\mathcal{N}}; \mu_0) &= \sum_{i=1}^{N_S} A_i(\boldsymbol{w}_i^{\mathcal{N}}, \boldsymbol{v}_i^{\mathcal{N}}; \mu_0) + \sum_{\{i,j \,|\, \Gamma_{ij} \neq \emptyset\}} \Big[-\mu_0 \left(\{\nabla \boldsymbol{w}^{\mathcal{N}}\}, [\![\boldsymbol{v}^{\mathcal{N}}]\!]\right)_{\Gamma_{ij}} - \mu_0 \left(\{\nabla \boldsymbol{v}^{\mathcal{N}}\}, [\![\boldsymbol{w}^{\mathcal{N}}]\!]\right)_{\Gamma_{ij}} \\
&\quad + \gamma\, \mu_0 \frac{p^2}{h} \left([\![\boldsymbol{w}^{\mathcal{N}}]\!], [\![\boldsymbol{v}^{\mathcal{N}}]\!]\right)_{\Gamma_{ij}} \Big], \\
B_{DG}(\boldsymbol{v}^{\mathcal{N}}, q^{\mathcal{N}}) &= \sum_{i=1}^{N_S} B_i(\boldsymbol{v}_i^{\mathcal{N}}, q_i^{\mathcal{N}}) + \sum_{\{i,j \,|\, \Gamma_{ij} \neq \emptyset\}} \left(\{q^{\mathcal{N}}\}, [\![\boldsymbol{v}^{\mathcal{N}}]\!]\right)_{\Gamma_{ij}},
\end{aligned}$$

for each $\boldsymbol{w}^{\mathcal{N}}$, $\boldsymbol{v}^{\mathcal{N}} \in V^{\mathcal{N}}$ and for each $q^{\mathcal{N}} \in Q^{\mathcal{N}}$. Standard DG-notation is used for the interface terms, namely on Γ_{ij} average and jump terms have the following meaning[3]:

$$\begin{aligned}
&\{\psi\} = \frac{\psi_i + \psi_j}{2}, && \text{if } \psi \text{ is a scalar or tensor-valued function,} \\
&[\![\boldsymbol{\tau}]\!] = \boldsymbol{\tau}_i \otimes \boldsymbol{n}_i + \boldsymbol{\tau}_j \otimes \boldsymbol{n}_j, \quad [\![\boldsymbol{\tau}]\!] = \boldsymbol{\tau}_i \cdot \boldsymbol{n}_i + \boldsymbol{\tau}_j \cdot \boldsymbol{n}_j && \text{if } \boldsymbol{\tau} \text{ is a vector-valued function,}
\end{aligned}$$

Finally, we introduce the global right-hand side functionals

$$F_{DG}(\boldsymbol{v}^{\mathcal{N}}; \boldsymbol{\mu}) = \sum_{i=1}^{N_S} F_i(\boldsymbol{v}_i^{\mathcal{N}}; \mu_0, \boldsymbol{\mu}_i), \quad G_{DG}(q^{\mathcal{N}}; \boldsymbol{\mu}) = \sum_{i=1}^{N_S} G_i(q_i^{\mathcal{N}}; \boldsymbol{\mu}_i).$$

Given $\boldsymbol{\mu} \in \mathcal{D}$, the high-fidelity approximation of the solution $(\boldsymbol{u}(\boldsymbol{\mu}), p(\boldsymbol{\mu}))$ of (1) is $(\boldsymbol{u}^{\mathcal{N}}(\boldsymbol{\mu}), p^{\mathcal{N}}(\boldsymbol{\mu})) \in V^{\mathcal{N}} \times Q^{\mathcal{N}}$ such that

$$\begin{aligned}
&A_{DG}(\boldsymbol{u}^{\mathcal{N}}(\boldsymbol{\mu}), \boldsymbol{v}^{\mathcal{N}}; \mu_0) + B_{DG}(\boldsymbol{v}^{\mathcal{N}}, p^{\mathcal{N}}(\boldsymbol{\mu})) = F_{DG}(\boldsymbol{v}^{\mathcal{N}}; \boldsymbol{\mu}) \quad \forall\, \boldsymbol{v}^{\mathcal{N}} \in V^{\mathcal{N}}, \\
&B_{DG}(\boldsymbol{u}^{\mathcal{N}}(\boldsymbol{\mu}), q^{\mathcal{N}}) = G_{DG}(q^{\mathcal{N}}; \boldsymbol{\mu}) \quad \forall\, q^{\mathcal{N}} \in Q^{\mathcal{N}}
\end{aligned} \tag{2}$$

Remark 2. We point out that we impose weakly the Dirichlet boundary datum, as customary in the DG context and sometimes also for conforming methods, see [26].

[3]Here the operator $\otimes$ is such that, given $\boldsymbol{a} = (a_1, a_2)^{\mathrm{T}}, \boldsymbol{b} = (b_1, b_2)^{\mathrm{T}} \in \mathbb{R}^2$, it holds $\boldsymbol{a} \otimes \boldsymbol{b} = \boldsymbol{a}\, \boldsymbol{b}^{\mathrm{T}} = \begin{pmatrix} a_1 b_1 & a_1 b_2 \\ a_2 b_1 & a_2 b_2 \end{pmatrix}$.

3.1. Well posedness of the high-fidelity approximation

In this section we investigate the well-posedness of problem (2), in particular we show that it admits a unique solution. The key ingredient is to prove an inf-sup condition for the bilinear form B_{DG}. We introduce the following local norms

$$\begin{aligned} \|\boldsymbol{v}_i^{\mathcal{N}}\|_{V_i^{\mathcal{N}}}^2 &= \|\boldsymbol{v}_i^{\mathcal{N}}\|_{H^1(\Omega_i)}^2 + \gamma \frac{p^2}{h} \left(\boldsymbol{v}_i^{\mathcal{N}}, \boldsymbol{v}_i^{\mathcal{N}}\right)_{\partial\Omega_i \cap \Sigma_D} \quad \forall\, \boldsymbol{v}_i^{\mathcal{N}} \in V_i^{\mathcal{N}}, \\ \|q_i^{\mathcal{N}}\|_{Q_i^{\mathcal{N}}}^2 &= \|q_i^{\mathcal{N}}\|_{L^2(\Omega_i)}^2 \qquad\qquad\qquad\qquad\quad \forall\, q_i^{\mathcal{N}} \in Q_i^{\mathcal{N}}, \end{aligned} \tag{3}$$

and the corresponding global ones

$$\begin{aligned} \|\boldsymbol{v}^{\mathcal{N}}\|_{V^{\mathcal{N}}}^2 &= \sum_{i=1}^{N_S} \|\boldsymbol{v}_i^{\mathcal{N}}\|_{V_i^{\mathcal{N}}}^2 + \gamma \frac{p^2}{h} \sum_{\{i,j \,|\, \Gamma_{ij} \neq \emptyset\}} \left(\llbracket \boldsymbol{v}^{\mathcal{N}} \rrbracket, \llbracket \boldsymbol{v}^{\mathcal{N}} \rrbracket\right)_{\Gamma_{ij}} \quad \forall\, \boldsymbol{v}^{\mathcal{N}} \in V^{\mathcal{N}}, \\ \|q^{\mathcal{N}}\|_{Q^{\mathcal{N}}}^2 &= \sum_{i=1}^{N_S} \|q_i^{\mathcal{N}}\|_{Q_i^{\mathcal{N}}}^2 \qquad\qquad\qquad\qquad\qquad\qquad\quad \forall\, q^{\mathcal{N}} \in Q^{\mathcal{N}}. \end{aligned} \tag{4}$$

By invoking [27, Th. 16.5], the well-posedness of the high-fidelity problem (2) is guaranteed by the following lemma.

Lemma 1. *Provided that the coefficient γ is large enough, there exists $K_B^{\mathcal{N}} > 0$ and for each $\boldsymbol{\mu} \in \mathcal{D}$ there exist $K_A^{\mathcal{N}}(\mu_0) > 0$, $K_F^{\mathcal{N}}(\boldsymbol{\mu}) > 0$ and $K_G^{\mathcal{N}}(\boldsymbol{\mu}) > 0$ such that*

$$|A_{DG}(\boldsymbol{w}^{\mathcal{N}}, \boldsymbol{v}^{\mathcal{N}}; \mu_0)| \leq K_A^{\mathcal{N}}(\mu_0) \|\boldsymbol{w}^{\mathcal{N}}\|_{V^{\mathcal{N}}} \|\boldsymbol{v}^{\mathcal{N}}\|_{V^{\mathcal{N}}} \quad \forall\, \boldsymbol{v}^{\mathcal{N}}, \boldsymbol{w}^{\mathcal{N}} \in V^{\mathcal{N}}, \tag{5}$$

$$|B_{DG}(\boldsymbol{v}^{\mathcal{N}}, q^{\mathcal{N}})| \leq K_B^{\mathcal{N}} \|\boldsymbol{v}^{\mathcal{N}}\|_{V^{\mathcal{N}}} \|q^{\mathcal{N}}\|_{Q^{\mathcal{N}}} \quad \forall\, q^{\mathcal{N}} \in Q^{\mathcal{N}}, \quad \forall\, \boldsymbol{v}^{\mathcal{N}} \in V^{\mathcal{N}}, \tag{6}$$

$$|F_{DG}(\boldsymbol{v}^{\mathcal{N}}; \boldsymbol{\mu})| \leq K_F^{\mathcal{N}}(\boldsymbol{\mu}) \|\boldsymbol{v}^{\mathcal{N}}\|_{V^{\mathcal{N}}} \quad \forall\, \boldsymbol{v}^{\mathcal{N}} \in V^{\mathcal{N}}, \tag{7}$$

$$|G_{DG}(q^{\mathcal{N}}; \boldsymbol{\mu})| \leq K_G^{\mathcal{N}}(\boldsymbol{\mu}) \|q^{\mathcal{N}}\|_{Q^{\mathcal{N}}} \quad \forall\, q^{\mathcal{N}} \in Q^{\mathcal{N}}. \tag{8}$$

Moreover, there exist $\alpha^{\mathcal{N}}(\mu_0) > 0$ and $\beta^{\mathcal{N}} > 0$ such that

$$\inf_{\boldsymbol{v}^{\mathcal{N}} \in V^{\mathcal{N}}} \frac{A_{DG}(\boldsymbol{v}^{\mathcal{N}}, \boldsymbol{v}^{\mathcal{N}}; \mu_0)}{\|\boldsymbol{v}^{\mathcal{N}}\|_{V^{\mathcal{N}}}^2} \geq \alpha^{\mathcal{N}}(\mu_0), \tag{9}$$

$$\inf_{q^{\mathcal{N}} \in Q^{\mathcal{N}}} \sup_{\boldsymbol{v}^{\mathcal{N}} \in V^{\mathcal{N}}} \frac{B_{DG}(\boldsymbol{v}^{\mathcal{N}}, q^{\mathcal{N}})}{\|\boldsymbol{v}^{\mathcal{N}}\|_{V^{\mathcal{N}}} \|q^{\mathcal{N}}\|_{Q^{\mathcal{N}}}} \geq \beta^{\mathcal{N}}. \tag{10}$$

Proof. Conditions (5), (6), (7) and (8) can be obtained using standard Cauchy-Schwarz inequalities, *cf.* [27], considering the following norms

$$\|\!|\boldsymbol{v}^{\mathcal{N}}|\!\|_{V^{\mathcal{N}}}^2 = \|\boldsymbol{v}^{\mathcal{N}}\|_{V^{\mathcal{N}}}^2 + \frac{h}{p^2} \sum_{i=1}^{N_S} \|\nabla \boldsymbol{v}_i^{\mathcal{N}}\|_{L^2(\partial\Omega_i)}^2, \quad \|\!|q^{\mathcal{N}}|\!\|_{Q^{\mathcal{N}}}^2 = \|q^{\mathcal{N}}\|_{Q^{\mathcal{N}}}^2 + \frac{h}{p^2} \sum_{i=1}^{N_S} \|q^{\mathcal{N}}\|_{L^2(\partial\Omega_i)}^2, \tag{11}$$

cf. [21], which allow to control the interface terms. However, the norms (11) are equivalent to those in (4) for $\boldsymbol{v}^{\mathcal{N}} \in V^{\mathcal{N}}$, $q^{\mathcal{N}} \in Q^{\mathcal{N}}$, thanks to standard inverse inequalities, *cf.* [21]. The coercivity condition (9) can be obtained as in the case of DG elliptic operators, *cf.* [28, 29, 30]. Let us focus on the inf-sup condition (10). First of all, we observe that we can rewrite it as: there exists $\beta^{\mathcal{N}} > 0$ such that

$$\forall\, q^{\mathcal{N}} \in Q^{\mathcal{N}} \quad \exists\, \boldsymbol{v}^{\mathcal{N}} \in V^{\mathcal{N}}, \quad \boldsymbol{v}^{\mathcal{N}} \neq 0, \quad \text{s. t.} \quad B_{DG}(\boldsymbol{v}^{\mathcal{N}}, q^{\mathcal{N}}) \geq \beta^{\mathcal{N}} \|\boldsymbol{v}^{\mathcal{N}}\|_{V^{\mathcal{N}}} \|q^{\mathcal{N}}\|_{Q^{\mathcal{N}}}. \tag{12}$$

Let $\widehat{K} = [-1, 1]^2$. It is known (see [31, Chap. IV, Prop. 7.2]) that $B_{\widehat{K}}(\boldsymbol{v}, q) = -(q, \operatorname{div} \boldsymbol{v})_{L^2(\widehat{K})}$ satisfies the inf-sup condition on the spaces $V_p^{\widehat{K}} = \mathbb{Q}_p(\widehat{K}) \cap [H_0^1(\widehat{K})]^2$, $Q_p^{\widehat{K}} = \mathbb{Q}_{p-2}(\widehat{K}) \cap L_0^2(\widehat{K})$ and the inf-sup constant

is $\beta_p^{\widehat{K}} \sim cp^{-1/2}$, with c independent of p. Thanks to our assumptions on the mesh (shape regularity in each Ω_i, global conformity and $p \geq 2$), by using Boland-Nicolaides arguments (*cf.* [32]) the form $B_\Omega(\boldsymbol{v}, q) = -(q, \operatorname{div} \boldsymbol{v})_{L^2(\Omega)}$ satisfies the inf-sup condition on the spaces $V^{\Omega,0} = \mathbb{Q}_p(\mathcal{T}_h) \cap [H_0^1(\Omega)]^2$, $Q^{\Omega,0} = \mathbb{Q}_{p-2}(\mathcal{T}_h) \cap L_0^2(\Omega)$, and the inf-sup constant is $\beta^{\Omega,0} = \beta_2^0 \left(\min_{K \in \mathcal{T}_h} \beta_p^K + 1\right)$ (where β_2^0 is the inf-sup constant of the couple $\mathbb{Q}_2 - \mathbb{Q}_0$ in Ω, while $\beta_p^K = c\beta_p^{\widehat{K}}$ for each $K \in \mathcal{T}_h$, with c independent of both p and meas(K), *cf.* [19, pag. 285]). By applying the arguments of [33, Prop 5.3.2], B_Ω satisfies the inf-sup condition on the spaces $V^\Omega = \mathbb{Q}_p(\mathcal{T}_h) \cap [H^1_{0,\Sigma_D}(\Omega)]^2$, $Q^\Omega = \mathbb{Q}_{p-2}(\mathcal{T}_h)$ and the inf-sup constant is $0 < \beta^\Omega < \beta^{\Omega,0}$, that is

$$\forall\, q^{\mathcal{N}} \in Q^\Omega \quad \exists\, \boldsymbol{w}^{\mathcal{N}} \in V^\Omega, \quad \boldsymbol{w}^{\mathcal{N}} \neq \boldsymbol{0} \quad \text{such that} \quad B_\Omega(\boldsymbol{w}^{\mathcal{N}}, q^{\mathcal{N}}) \geq \beta^\Omega \, \|\boldsymbol{w}^{\mathcal{N}}\|_{H^1(\Omega)} \, \|q^{\mathcal{N}}\|_{Q^{\mathcal{N}}}.$$

As $\boldsymbol{w}^{\mathcal{N}} \in V^\Omega$, it is continuous on Ω and null on Σ_D and it holds that

$$\|\boldsymbol{w}^{\mathcal{N}}\|_{V^{\mathcal{N}}} = \|\boldsymbol{w}^{\mathcal{N}}\|_{H^1(\Omega)} \quad \text{and} \quad B_{DG}(\boldsymbol{w}^{\mathcal{N}}, q^{\mathcal{N}}) = B_\Omega(\boldsymbol{w}^{\mathcal{N}}, q^{\mathcal{N}}) \quad \forall\, q^{\mathcal{N}} \in Q^{\mathcal{N}},$$

because the interface and boundary terms vanish. Recalling that $Q^{\mathcal{N}} = Q^\Omega$, we can now obtain (12) with $\beta^{\mathcal{N}} = \beta^\Omega$ by taking $\boldsymbol{v}^{\mathcal{N}} = \boldsymbol{w}^{\mathcal{N}}$.

Remark 3. In case of geometrical parameters, $\Omega = \Omega(\boldsymbol{\mu})$ and the bilinear form B_{DG} become parameter dependent [34]. The inf-sup condition (10) still holds true, however with a $\boldsymbol{\mu}$-dependent constant $\beta^{\mathcal{N}}(\boldsymbol{\mu})$. The proof follows by using the same arguments of Lemma 1. The main difference is that the global mesh to be considered is $T^{\boldsymbol{\mu}}(\mathcal{T}_h)$, the image through the geometrical transformation $T^{\boldsymbol{\mu}} \colon \Omega \to \Omega(\boldsymbol{\mu})$ of a regular mesh $\mathcal{T}_h$ defined on a reference domain Ω. The map $T^{\boldsymbol{\mu}}$ is assumed to be sufficiently regular in order to ensure the needed regularity properties of $T^{\boldsymbol{\mu}}(\mathcal{T}_h)$.

4. DGRBE approximation

In this section we present our Discontinuous Galerkin Reduced Basis Element (DGRBE) method that extends the method proposed in [1] for elliptic equations. The main novelty of the present work consists in introducing basis enrichment techniques in order to guarantee the inf-sup stability for the reduced problem.

Like most of the reduced basis methods, *cf.* [2], our DGRBE method is built on two computational stages, one offline, the other online. During the offline stage (typically expensive) we build low-dimensional local approximation spaces V_i^{RB} and Q_i^{RB} spanned by a small number of high-fidelity solutions of local Stokes problems computed in correspondence of N_i parameters selected by the Greedy algorithm [2]. Then, for any given new value of the parameter $\boldsymbol{\mu} \in \mathcal{D}$, the global reduced approximate solution of (1) is computed in the (inexpensive) online stage.

Remark 4. We assume that our bilinear and linear forms depend "affinely" on the parameter $\boldsymbol{\mu}$, *cf.* [2]. In the particular case of the DGRBE, this requirement is discussed in [1, Appendix A] together with the implementation details.

4.1. Local reduced spaces construction

The construction of the reduced spaces is made independently on each subdomain using a standard RB Greedy algorithm [34]. In our case the computational cost of this operation does not depend on the dimensions $\mathcal{N}^V$, $\mathcal{N}^Q$ of the global high-fidelity spaces , but only on that of the local ones, *i.e.* $\mathcal{N}_i^V$, $\mathcal{N}_i^Q$.

Let us focus on the generic subdomain Ω_i. The method used to build $V_i^{\mathcal{N}}$ and $Q_i^{\mathcal{N}}$ is similar to the one presented in [1], which is based on the introduction of an additional discrete parameter η whose role is to select different functions to be used as Neumann data on the boundary regions $\Gamma_i = \partial\Omega_i \backslash \partial\Omega$. Under the assumption that Γ_i is the union of straight segments Γ_{ij}, these functions are set null on Γ_i except on one segment Γ_{ij} where they are Legendre polynomials of degree $s \leq M_i$, as in the so-called "Method B" of [1]. Since the Legendre polynomials form a complete basis of $L^2(-1, 1)$, we expect that using these polynomials up to degree M_i to reproduce the unknown normal component of the Cauchy stress tensor of the exact

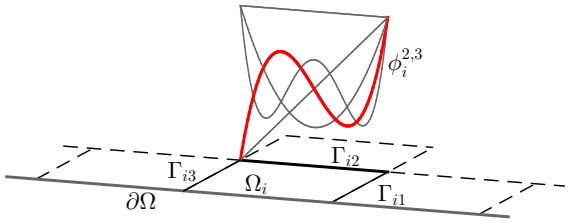

Figure 1: Definition of the parameters η following the formulas (14). In the example we take $M_i = 4$ (the maximum polynomial degree), Γ_i is formed by $N_{J_i} = 3$ segments, we take $j = 2$ and $s = 3$. Starting from the Legendre polynomial $\phi_i^{2,3}$ (red line) we have $\eta = 17$ (for $k = 1$) and $\eta = 18$ (for $k = 2$)

global solution across the interface Γ_i will provide an accurate system of snapshots in the reduced basis, either of local (in Ω_i) or global (in Ω) type.

We denote with $\mathcal{D}_i^{BC} \subset \mathbb{N}$ the set in which η takes values. We then define the extended parameter space $\mathcal{D}_i^{ext} = \mathcal{D}_0 \times \mathcal{D}_i \times \mathcal{D}_i^{BC}$ and denote with $\widetilde{\boldsymbol{\mu}}_i = (\mu_0, \boldsymbol{\mu}_i, \eta)$ its generic element. Then, let $(\widetilde{\boldsymbol{u}}_i^{\mathcal{N}}(\widetilde{\boldsymbol{\mu}}_i), \widetilde{p}_i^{\mathcal{N}}(\widetilde{\boldsymbol{\mu}}_i)) \in V_i^{\mathcal{N}} \times Q_i^{\mathcal{N}}$ be the solution of

$$\begin{aligned} &A_i(\widetilde{\boldsymbol{u}}_i^{\mathcal{N}}(\widetilde{\boldsymbol{\mu}}_i), \boldsymbol{v}_i^{\mathcal{N}}; \mu_0) + B_i(\boldsymbol{v}_i^{\mathcal{N}}, \widetilde{p}_i^{\mathcal{N}}(\widetilde{\boldsymbol{\mu}}_i)) = \delta_{0,\eta}\, F_i(\boldsymbol{v}_i^{\mathcal{N}}; \mu_0, \boldsymbol{\mu}_i) + \langle \mathcal{I}_i^{\eta}, \boldsymbol{v}_i^{\mathcal{N}} \rangle \quad && \forall\, \boldsymbol{v}_i^{\mathcal{N}} \in V_i^{\mathcal{N}}, \\ &B_i(\widetilde{\boldsymbol{u}}_i^{\mathcal{N}}(\widetilde{\boldsymbol{\mu}}_i), q_i^{\mathcal{N}}) = \delta_{0,\eta}\, G_i(q_i^{\mathcal{N}}; \boldsymbol{\mu}_i) && \forall\, q_i^{\mathcal{N}} \in Q_i^{\mathcal{N}}, \end{aligned} \tag{13}$$

where $\delta_{a,b}$ denotes the Kronecker delta and the functional $\mathcal{I}_i^{\eta}$ has the role to impose a Neumann boundary condition on Γ_i . When $\eta = 0$, we set $\mathcal{I}_i^{\eta} = 0$, thus problem (13) has homogeneous Neumann conditions on the Γ_i. To precisely define the functional $\mathcal{I}_i^{\eta}$ when $\eta \neq 0$, let us introduce the set $J_i = \{j \,|\, \overline{\Omega}_i \cap \overline{\Omega}_j \neq \emptyset\}$ and assume that each interface Γ_{ij}, $j \in J_i$, is a straight segment so that there exists an affine map $T_{\Gamma_{ij}} : [-1, 1] \to \Gamma_{ij}$. We denote with N_{J_i} the number of elements of J_i and for the sake of exposition we assume that $J_i = \{1, \ldots, N_{J_i}\}$. We then denote with $\widehat{\phi}_s$ the Legendre polynomial of degree s defined on $[-1, 1]$ and $\phi_i^{j,s} = \widehat{\phi}_s \circ T_{\Gamma_{ij}}^{-1}$. We set M_i as the maximum admissible degree for the Legendre polynomials and define the additional parameter space $\mathcal{D}_i^{BC} = \{0, \ldots, 2\, N_{J_i}(M_i + 1)\}$. We point out that the value M_i is set *a priori* during the offline stage. At the moment the convergence analysis of DGRBE for the Stokes problem is in progress, thus a rule to choose M_i is not available yet. Nevertheless, we propose a possible strategy to set M_i that consists in selecting the minimum polynomial degree such that the ratio between the RB error and the high-fidelity one, tested on a set of random parameters, is less than 10 (see Sect. 5). Let us denote with $(\cdot, \cdot)_{\Gamma_{ij}}$ the L^2 inner product on Γ_{ij}, then (when $\eta \neq 0$) we define the functionals $\mathcal{I}_i^{\eta}$ as follows:

$$\begin{array}{l} \text{for } j = 1, \ldots, N_{J_i} \qquad (j \text{ identifies the segment } \Gamma_{ij}) \\ \quad \text{for } s = 0, \ldots, M_i \qquad (s \text{ is the degree of the Legendre polynomial on } \Gamma_{ij}) \\ \quad\quad \text{for } k = 1, 2 \qquad (k \text{ identifies the vector component}) \\ \quad\quad\quad \text{set } \eta = 2(M_i + 1)(j - 1) + 2s + k \\ \quad\quad\quad \text{set } \langle \mathcal{I}_i^{\eta}, \boldsymbol{v}^{\mathcal{N}} \rangle = \begin{cases} \left(\begin{pmatrix} \phi_i^{j,s} \\ 0 \end{pmatrix}, \boldsymbol{v}^{\mathcal{N}} \right)_{\Gamma_{ij}} & \text{if } k = 1 \\ \left(\begin{pmatrix} 0 \\ \phi_i^{j,s} \end{pmatrix}, \boldsymbol{v}^{\mathcal{N}} \right)_{\Gamma_{ij}} & \text{if } k = 2 \end{cases} \end{array} \tag{14}$$

In this way, the parameters η are defined univocally in each subdomain (see Fig. 1). All these combinations allow us to approximate in a very effective way the normal component of the Cauchy stress tensor of the global solution $(\boldsymbol{u}^{\mathcal{N}}(\boldsymbol{\mu}), p^{\mathcal{N}}(\boldsymbol{\mu}))$, that is not known during the local offline computation.

During the Greedy procedure a set of values of parameters $S_i = \{\widetilde{\boldsymbol{\mu}}_i^1, \ldots, \widetilde{\boldsymbol{\mu}}_i^{N_i}\} \subset \mathcal{D}_i^{ext}$ is selected and

the following spaces are built (for details on the algorithm see [35])

$$V_i^{RB} = \text{span}(\{\widetilde{\boldsymbol{u}}_i^{\mathcal{N}}(\widetilde{\boldsymbol{\mu}}_i^1), \dots, \widetilde{\boldsymbol{u}}_i^{\mathcal{N}}(\widetilde{\boldsymbol{\mu}}_i^{N_i})\} \cup \{\widetilde{\boldsymbol{\sigma}}_i^{\mathcal{N}}(\widetilde{\boldsymbol{\mu}}_i^1), \dots, \widetilde{\boldsymbol{\sigma}}_i^{\mathcal{N}}(\widetilde{\boldsymbol{\mu}}_i^{N_i})\}),$$
$$Q_i^{RB} = \text{span}\{\widetilde{p}_i^{\mathcal{N}}(\widetilde{\boldsymbol{\mu}}_i^1), \dots, \widetilde{p}_i^{\mathcal{N}}(\widetilde{\boldsymbol{\mu}}_i^{N_i})\}.$$

Here $\widetilde{\boldsymbol{\sigma}}_i^{\mathcal{N}}(\widetilde{\boldsymbol{\mu}}_i^k)$, $k = 1, \dots, N_i$, are the *supremizers*, see *e.g.* [17]. They are defined as

$$\widetilde{\boldsymbol{\sigma}}_i^{\mathcal{N}}(\widetilde{\boldsymbol{\mu}}_i^k) \in V_i^{\mathcal{N}} : \quad (\widetilde{\boldsymbol{\sigma}}_i^{\mathcal{N}}(\widetilde{\boldsymbol{\mu}}_i^k), \boldsymbol{v}_i^{\mathcal{N}})_{V_i^{\mathcal{N}}} = B_i(p_i^{\mathcal{N}}(\widetilde{\boldsymbol{\mu}}_i^k), \boldsymbol{v}_i^{\mathcal{N}}) \quad \forall\, \boldsymbol{v}_i^{\mathcal{N}} \in V_i^{\mathcal{N}}, \tag{15}$$

where $(\cdot,\cdot)_{V_i^{\mathcal{N}}}$ is the inner product associated with the norm $\|\cdot\|_{V_i^{\mathcal{N}}}$ defined in (3). The supremizers are added in order to ensure the inf-sup stability of the reduced problem

$$\begin{aligned} &A_i(\widetilde{\boldsymbol{u}}_i^{RB}(\widetilde{\boldsymbol{\mu}}_i), \boldsymbol{v}_i^{RB}; \mu_0) + B_i(\boldsymbol{v}_i^{RB}, \widetilde{p}_i^{RB}(\widetilde{\boldsymbol{\mu}}_i)) = \delta_{0,\eta}\, F_i(\boldsymbol{v}_i^{RB}; \mu_0, \boldsymbol{\mu}_i) + \langle \mathcal{I}_i^\eta, \boldsymbol{v}_i^{RB} \rangle \quad \forall\, \boldsymbol{v}_i^{RB} \in V_i^{RB}, \\ &B_i(\widetilde{\boldsymbol{u}}_i^{RB}(\widetilde{\boldsymbol{\mu}}_i), q_i^{RB}) = \delta_{0,\eta}\, G_i(q_i^{RB}; \boldsymbol{\mu}_i) \quad \forall\, q_i^{RB} \in Q_i^{RB}. \end{aligned} \tag{16}$$

Finally, we would like to point out that the Greedy algorithm terminates when

$$\|r_i\left(\cdot; (\widetilde{\boldsymbol{u}}_i^{RB}(\widetilde{\boldsymbol{\mu}}_i), \widetilde{p}_i^{RB}(\widetilde{\boldsymbol{\mu}}_i)\right), \widetilde{\boldsymbol{\mu}}_i)\|_{(V_i^{\mathcal{N}} \times Q_i^{\mathcal{N}})'} / \|\mathcal{F}(\cdot)\|_{(V_i^{\mathcal{N}} \times Q_i^{\mathcal{N}})'} \le \varepsilon^* \quad \forall \widetilde{\boldsymbol{\mu}}_i \in \Xi_i \subset \mathcal{D}_i^{ext}, \tag{17}$$

where ε^* is a given tolerance, $\mathcal{F}(\cdot)$ is the right hand side of system (16), and $r_i\left(\cdot; (\widetilde{\boldsymbol{u}}_i^{RB}(\widetilde{\boldsymbol{\mu}}_i), \widetilde{p}_i^{RB}(\widetilde{\boldsymbol{\mu}}_i)), \widetilde{\boldsymbol{\mu}}_i\right) : V^{\mathcal{N}} \times Q^{\mathcal{N}} \to \mathbb{R}$ is the residual of (13), *i.e.*

$$\begin{aligned} r_i\left((\boldsymbol{v}_i^{\mathcal{N}}, q_i^{\mathcal{N}}); (\widetilde{\boldsymbol{u}}_i^{RB}(\widetilde{\boldsymbol{\mu}}_i), \widetilde{p}_i^{RB}(\boldsymbol{\mu}_i)), \widetilde{\boldsymbol{\mu}}_i\right) &= \delta_{0,\eta}\, F_i(\boldsymbol{v}_i^{\mathcal{N}}; \mu_0, \boldsymbol{\mu}_i) + \langle \mathcal{I}_i^\eta, \boldsymbol{v}_i^{\mathcal{N}} \rangle - A_i(\widetilde{\boldsymbol{u}}_i^{RB}(\widetilde{\boldsymbol{\mu}}_i), \boldsymbol{v}_i^{\mathcal{N}}; \mu_0) \\ &\quad + B_i(\boldsymbol{v}_i^{\mathcal{N}}, \widetilde{p}_i^{RB}(\widetilde{\boldsymbol{\mu}}_i)) + \delta_{0,\eta}\, G_i(q_i^{\mathcal{N}}; \boldsymbol{\mu}_i) - B_i(\widetilde{\boldsymbol{u}}_i^{RB}(\widetilde{\boldsymbol{\mu}}_i), q_i^{\mathcal{N}}). \end{aligned}$$

The discrete set Ξ_i in (17) is the so-called training set used to perform the Greedy procedure. As a result of the Greedy algorithm, some $\eta \in \{0, \dots, 2N_{J_i}(M_i + 1)\}$ can be missing in the $\widetilde{\boldsymbol{\mu}}_i^k$ when h is large, p is small and $M_i \gg p$ (as a consequence of the fact that the high-fidelity space is very small and the RB space rapidly tends to it during the Greedy algorithm), otherwise in general all the η are present as components of the $\widetilde{\boldsymbol{\mu}}_i^k$, for $k = 1, \dots, N_i$.

4.2. Global reduced solution

We define the global reduced spaces as

$$V^{RB} = \bigoplus_{i=1}^{N_S} V_i^{RB}, \quad Q^{RB} = \bigoplus_{i=1}^{N_S} Q_i^{RB}.$$

We denote with N_i^V, N^V, N_i^Q, N^Q the dimensions of V_i^{RB}, V^{RB}, Q_i^{RB}, Q^{RB}, respectively. We require, for $i = 1, \dots, N_S$, that $N_i^V \ll \mathcal{N}_i^V$ and $N_i^Q \ll \mathcal{N}_i^Q$, where $\mathcal{N}_i^V$ and $\mathcal{N}_i^Q$ are the dimensions of $V_i^{\mathcal{N}}$ and $Q_i^{\mathcal{N}}$. Once we have the global reduced spaces, we can project our problem in order to rapidly compute the reduced solution. The DGRBE approximation $(\boldsymbol{u}^{RB}(\boldsymbol{\mu}), p^{RB}(\boldsymbol{\mu})) \in V^{RB} \times Q^{RB}$ then satisfies the Galerkin problem:

$$\begin{aligned} &A_{DG}(\boldsymbol{u}^{RB}(\boldsymbol{\mu}), \boldsymbol{v}^{RB}; \mu_0) + B_{DG}(\boldsymbol{v}^{RB}, p^{RB}(\boldsymbol{\mu})) = F_{DG}(\boldsymbol{v}^{RB}; \boldsymbol{\mu}) \quad \forall\, \boldsymbol{v}^{RB} \in V^{RB}, \\ &B_{DG}(\boldsymbol{u}^{RB}(\boldsymbol{\mu}), q^{RB}) = G_{DG}(q^{RB}; \boldsymbol{\mu}) \quad \forall\, q^{RB} \in Q^{RB}. \end{aligned} \tag{18}$$

We observe that the algebraic problem associated with (18) has dimensions $(N^V + N^Q)$, hence it is much smaller than the dimension of the high-fidelity problem, that is $(\mathcal{N}^V + \mathcal{N}^Q)$. Note that the DGRBE approximation (18) is the projection of (2) onto the reduced space $V^{RB} \times Q^{RB}$.

Remark 5. Differently from the elliptic case studied in [1], here the well-posedness of the reduced problem is not inherited from the high-fidelity one. Nevertheless, the use of supremizers introduced in (15) ensures that the bilinear form B_{DG} satisfies the inf-sup condition

$$\inf_{q^{RB} \in Q^{RB}} \sup_{\boldsymbol{v}^{RB} \in V^{RB}} \frac{B_{DG}(\boldsymbol{v}^{RB}, q^{RB})}{\|q^{RB}\|_{Q^{\mathcal{N}}}\, \|\boldsymbol{v}^{RB}\|_{V^{\mathcal{N}}}} = \beta^{RB} > 0. \tag{19}$$

Although not rigorously proved, experiments show that, with our approach, condition (19) is numerically satisfied, as we will see in Section 5.

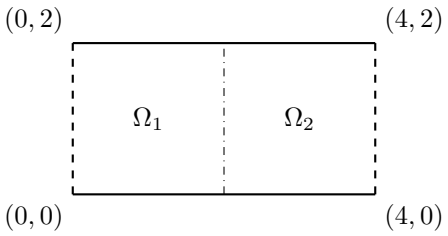

Figure 2: Computational domain Ω considered in the numerical tests. The continuous line corresponds to Dirichlet boundary conditions, while the dashed line to the Neumann ones.

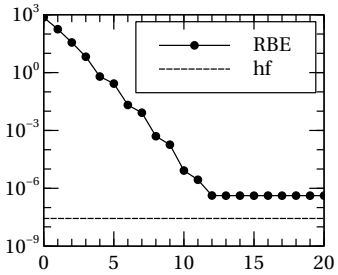

Figure 3: DGRBE error $\|\boldsymbol{u}(\boldsymbol{\mu}) - \boldsymbol{u}^{RB}(\boldsymbol{\mu})\|_{V^{\mathcal{N}}}$ (RBE) and hi-fi error $\|\boldsymbol{u}(\boldsymbol{\mu}) - \boldsymbol{u}^{\mathcal{N}}(\boldsymbol{\mu})\|_{V^{\mathcal{N}}}$ (hf) versus M_i. Here $h = 1/32$ and $N = 6$. The errors are an average over a sample of 20 random parameter values.

5. Numerical results

In this section we provide numerical verification of the method presented in the previous sections. We consider the domain $\Omega = (0,4) \times (0,2)$, partitioned into $\Omega_1 = (0,2) \times (0,2)$ and $\Omega_2 = (2,4) \times (0,2)$. The domain is sketched in Figure 2. The right-hand side functional of (1) and the boundary conditions are chosen in order to obtain that the exact solution is

$$\boldsymbol{u}(\boldsymbol{\mu})(x,y) = \begin{pmatrix} \mu^1(-e^x(y\cos y + \sin y)) + \mu^2 e^{x+y}, \\ \mu^1(e^x y \sin y) + \mu^2(-e^{x+y}) \end{pmatrix}, \quad p(\boldsymbol{\mu})(x,y) = \mu^1(2\,e^x \sin y) - \mu^2 \pi\, \cos(\pi\, x)\, \cos(\pi\, y).$$

Here we do not have local parameters, but only global ones. Thus, we set $\mathcal{D}_1 = \mathcal{D}_2 = [0,1]^2$ and in the setting defined in Section 2, the parameter space $\mathcal{D}$ can be expressed as $\mathcal{D} = \{(\boldsymbol{\mu}_1, \boldsymbol{\mu}_2) \in \mathcal{D}_1 \times \mathcal{D}_2 \,|\, \mu_1^1 = \mu_2^1, \quad \mu_1^2 = \mu_2^2\}$ where $\boldsymbol{\mu}_i = (\mu_i^1, \mu_i^2) \quad i = 1,2$. We set $\mu_0 = 1$, actually we are not considering the viscosity as a parameter. The aim of this experiment is to investigate the conditions in which our reduced strategy yields significant computational savings without losing accuracy. We applied the DGRBE method to the SEM high-fidelity (hi-fi) discretization with mesh size h and polynomials degree p. We performed the Greedy algorithm using a tolerance $\varepsilon^* = 10^{-5}$ and the value of M_i shown in Table 1 (which is set *a priori* in the offline stage). More precisely, for each couple (h,p), we choose (*a priori*) the minimum value of M_i, $i = 1,2$, s.t. $\max\{\overline{E}_r^V, \overline{E}_r^Q\} \leq 10$, being $\overline{E}_r^V$ and $\overline{E}_r^Q$ the average over a sample of 20 random parameter values of

$$E_r^V(\boldsymbol{\mu}) = \frac{\|\boldsymbol{u}(\boldsymbol{\mu}) - \boldsymbol{u}^{RB}(\boldsymbol{\mu})\|_{V^{\mathcal{N}}}}{\|\boldsymbol{u}(\boldsymbol{\mu}) - \boldsymbol{u}^{\mathcal{N}}(\boldsymbol{\mu})\|_{V^{\mathcal{N}}}} \quad \text{and} \quad E_r^Q(\boldsymbol{\mu}) = \frac{\|p(\boldsymbol{\mu}) - p^{RB}(\boldsymbol{\mu})\|_{Q^{\mathcal{N}}}}{\|p(\boldsymbol{\mu}) - p^{\mathcal{N}}(\boldsymbol{\mu})\|_{Q^{\mathcal{N}}}},$$

respectively. This means that the average error of the DGRBE approximation can be at most one order of magnitude higher than the average hi-fi error. The optimal value of M_i has been determined by multiple experiments. In some cases (those corresponding to the starred values in Table 1) the desired accuracy cannot be reached by increasing M_i. In Figure 3 we show the behaviour of $\|\boldsymbol{u}(\boldsymbol{\mu}) - \boldsymbol{u}^{RB}(\boldsymbol{\mu})\|_{V^{\mathcal{N}}}$ versus M_i and we compare it with $\|\boldsymbol{u}(\boldsymbol{\mu}) - \boldsymbol{u}^{\mathcal{N}}(\boldsymbol{\mu})\|_{V^{\mathcal{N}}}$, in the case $h = 1/32$ and $N = 6$. We observe that there is a plateau. The plateau is a consequence of the fact that the local spaces built by the Greedy procedure are able to reproduce the hi-fi approximation only up to a value related to the tolerance ε^*. In Table 2 we compare the dimension of both the SEM hi-fi discretization and that of the DGRBE one.

In Table 3 we show the computational speed-up, *i.e.*, the ratio between the computational time T_{hf} of the hi-fi model and the one T_{on} of the online stage of the DGRBE. Moreover, we analyse the trade-off, that is the number N_{to} of online simulations to be performed in order to have an effective advantage w.r.t. solve N_{to} hi-fi problems. It is computed as $N_{\text{to}} = \frac{T_{\text{off}}}{T_{\text{hf}} - T_{\text{on}}}$, where T_{off} is the computational time of the offline stage. A significant computational speed-up is obtained even guaranteeing that the accuracy of the DGRBE approximation and the hi-fi one are comparable, provided that we are able to choose a suitable maximum degree M_i of the Legendre interface conditions that grows w.r.t. both p and $1/h$. From this simple test case

	$p=2$	$p=3$	$p=4$	$p=5$	$p=6$	$p=7$	$p=8$
$h=1$	-1	0	1	2	3	4	5
$h=1/2$	-1	1	2	3	4	6	8
$h=1/4$	0	2	3	5	6	8	10
$h=1/8$	0	2	4	6	8	10	12
$h=1/16$	1	3	6	8	10	12	20^*
$h=1/32$	2	5	8	20^*	20^*	20^*	20^*

Table 1: Minimum value of M_i for which it holds $\max\{E_r^V(\boldsymbol{\mu}), E_r^Q(\boldsymbol{\mu})\} \leq 10$. The value -1 means that no Legendre interface conditions are used. The superscript * means that the tolerance on the ratio has not been reached.

	$p=2$	$p=3$	$p=4$	$p=5$	$p=6$	$p=7$	$p=8$
$h=1$	38/8	72/24	118/36	176/48	246/60	328/72	422/84
$h=1/2$	108/12	228/36	396/48	612/60	876/72	1188/96	1548/120
$h=1/4$	356/24	804/48	1444/60	2276/84	3300/96	4516/120	5924/144
$h=1/8$	1284/24	3012/48	5508/72	8772/96	12804/120	17604/144	23172/168
$h=1/16$	4868/36	11652/60	21508/96	34436/120	50436/144	69508/168	91652/264
$h=1/32$	18948/48	45828/84	84996/120	136452/264	200196/264	276228/264	364548/264

Table 2: Spaces dimensions. We compare here the dimension of the hi-fi space $V_i^{\mathcal{N}} \times Q_i^{\mathcal{N}}$ (on the left) with the dimension of the DGRBE space $V^{RB} \times Q^{RB}$ (on the right), built by using the M_i shown in Table 1.

it turns out that both the speed-up and the trade-off are better for those values of p and h corresponding to the lower triangle of the blocks in Table 3, *i.e.*, the larger p, the larger h.

Finally in Table 4 we show the discrete inf-sup constant for both the hi-fi and the DGRBE model. These values have been computed by solving the generalized eigenproblem shown in, *e.g.*, [36]. We observe that the supremizer enrichment allows to recover good stability properties for the reduced problem. The data shown in Tables 3 and 4 are averaged over a sample of 20 parameter values.

6. Conclusions

We proposed an extension of the DGRBE method [1] for Stokes problem. The high-fidelity model is based on spectral elements approximation. The basis functions are discontinuous along the subdomain interfaces and the DG approach has been followed in order to recover the continuity of the velocities and of the normal component of the Cauchy stress tensor. We proved the well-posedness of the high-fidelity approximation. We then introduced the reduced model and proposed a space enrichment technique in order to recover the inf-sup stability of the reduced model, which is not rigorously proven but it is numerically evident. In the numerical tests we have analysed how the accuracy of the DGRBE approximation depends on the maximum degree M_i of the Legendre polynomials used as interface conditions during the offline stage. We also assessed that the DGRBE approach provides significant computational savings in a certain range of the discretization parameters (h, p), and the larger p, the larger h.

Further work should be devoted to improve the space enrichment technique as well as to develop an effective *a posteriori* error estimator for the certification of the global reduced solution.

References

[1] P. F. Antonietti, P. Pacciarini, A. Quarteroni, A discontinuous Galerkin reduced basis element method for elliptic problems, ESAIM: M2AN (2015). In press. doi:10.1051/m2an/2015045.

[2] A. Manzoni, F. Negri, A. Quarteroni, Reduced Basis Methods for Partial Differential Equations, Springer, 2015.

[3] Y. Maday, E. M. Rønquist, A reduced-basis element method, in: Proceedings of the Fifth International Conference on Spectral and High Order Methods (ICOSAHOM-01) (Uppsala), Vol. 17, 2002, pp. 447–459.

[4] Y. Maday, E. M. Rønquist, The reduced basis element method: application to a thermal fin problem, SIAM J. Sci. Comput. 26 (1) (2004) 240–258.

	$p=2$	$p=3$	$p=4$	$p=5$	$p=6$	$p=7$	$p=8$
$h=1$	$4.59\cdot10^{0}$	$1.55\cdot10^{0}$	$1.90\cdot10^{0}$	$2.47\cdot10^{0}$	$3.49\cdot10^{0}$	$4.65\cdot10^{0}$	$7.10\cdot10^{0}$
$h=1/2$	$1.68\cdot10^{0}$	$2.57\cdot10^{0}$	$4.51\cdot10^{0}$	$7.61\cdot10^{0}$	$1.16\cdot10^{1}$	$1.74\cdot10^{1}$	$1.91\cdot10^{1}$
$h=1/4$	$2.75\cdot10^{0}$	$6.79\cdot10^{0}$	$1.44\cdot10^{1}$	$2.11\cdot10^{1}$	$3.84\cdot10^{1}$	$5.37\cdot10^{1}$	$7.11\cdot10^{1}$
$h=1/8$	$7.49\cdot10^{0}$	$3.24\cdot10^{1}$	$6.49\cdot10^{1}$	$1.19\cdot10^{2}$	$1.79\cdot10^{2}$	$2.79\cdot10^{2}$	$3.58\cdot10^{2}$
$h=1/16$	$3.73\cdot10^{1}$	$1.92\cdot10^{2}$	$4.02\cdot10^{2}$	$7.22\cdot10^{2}$	$1.16\cdot10^{3}$	$1.83\cdot10^{3}$	
$h=1/32$	$3.22\cdot10^{2}$	$1.28\cdot10^{3}$	$2.91\cdot10^{3}$				
$h=1$	$1.83\cdot10^{2}$	$1.35\cdot10^{3}$	$8.09\cdot10^{2}$	$1.00\cdot10^{3}$	$1.48\cdot10^{3}$	$1.03\cdot10^{3}$	$7.08\cdot10^{2}$
$h=1/2$	$8.02\cdot10^{2}$	$4.86\cdot10^{2}$	$9.50\cdot10^{2}$	$6.48\cdot10^{2}$	$4.18\cdot10^{2}$	$3.83\cdot10^{2}$	$4.51\cdot10^{2}$
$h=1/4$	$5.99\cdot10^{2}$	$6.69\cdot10^{2}$	$3.92\cdot10^{2}$	$3.47\cdot10^{2}$	$2.70\cdot10^{2}$	$3.08\cdot10^{2}$	$3.49\cdot10^{2}$
$h=1/8$	$6.77\cdot10^{2}$	$2.19\cdot10^{2}$	$1.87\cdot10^{2}$	$7.43\cdot10^{1}$	$6.98\cdot10^{1}$	$8.20\cdot10^{1}$	$1.02\cdot10^{2}$
$h=1/16$	$2.24\cdot10^{2}$	$6.59\cdot10^{1}$	$5.16\cdot10^{1}$	$5.06\cdot10^{1}$	$5.17\cdot10^{1}$	$6.16\cdot10^{1}$	
$h=1/32$	$9.89\cdot10^{1}$	$4.01\cdot10^{1}$	$3.44\cdot10^{1}$				

Table 3: Computational speed-up $\frac{T_{\text{hf}}}{T_{\text{on}}}$ (top block) and Trade-off $N_{\text{to}} = \frac{T_{\text{off}}}{T_{\text{hf}}-T_{\text{on}}}$ (bottom block). We show only the (h,p) couples satisfying the accuracy condition $\max\{E_r^V(\boldsymbol{\mu}), E_r^Q(\boldsymbol{\mu})\} \leq 10$.

	$p=2$	$p=4$	$p=6$	$p=8$
$h=1$	$7.18\cdot10^{-1}/7.18\cdot10^{-1}$	$4.13\cdot10^{-1}/4.11\cdot10^{-1}$	$3.99\cdot10^{-1}/3.99\cdot10^{-1}$	$3.98\cdot10^{-1}/3.98\cdot10^{-1}$
$h=1/2$	$5.25\cdot10^{-1}/5.24\cdot10^{-1}$	$4.00\cdot10^{-1}/4.00\cdot10^{-1}$	$3.99\cdot10^{-1}/3.98\cdot10^{-1}$	$3.98\cdot10^{-1}/3.81\cdot10^{-1}$
$h=1/4$	$4.39\cdot10^{-1}/4.38\cdot10^{-1}$	$3.99\cdot10^{-1}/3.81\cdot10^{-1}$	$3.98\cdot10^{-1}/2.79\cdot10^{-1}$	$3.98\cdot10^{-1}/1.97\cdot10^{-1}$
$h=1/8$	$4.11\cdot10^{-1}/2.30\cdot10^{-1}$	$3.99\cdot10^{-1}/2.41\cdot10^{-1}$	$3.98\cdot10^{-1}/1.56\cdot10^{-1}$	$3.98\cdot10^{-1}/9.88\cdot10^{-2}$
$h=1/16$	$4.02\cdot10^{-1}/2.29\cdot10^{-1}$	$3.99\cdot10^{-1}/1.95\cdot10^{-1}$	$3.98\cdot10^{-1}/1.24\cdot10^{-1}$	$3.98\cdot10^{-1}/1.44\cdot10^{-1}$

Table 4: Discrete inf-sup constant. The value on the left refers to the hi-fi model, the value on the right to the DGRBE one.

[5] A. E. Løvgren, Y. Maday, E. M. Rønquist, A reduced basis element method for the steady Stokes problem, M2AN Math. Model. Numer. Anal. 40 (3) (2006) 529–552.

[6] A. E. Løvgren, Y. Maday, E. M. Rønquist, A reduced basis element method for the steady Stokes problem: application to hierarchical flow systems, Model. Identif. Control 27 (2) (2006) 79–94.

[7] L. Iapichino, A. Quarteroni, G. Rozza, A reduced basis hybrid method for the coupling of parametrized domains represented by fluidic networks, Comput. Methods Appl. Mech. Engrg. 221/222 (2012) 63–82.

[8] Y. Chen, J. S. Hesthaven, Y. Maday, A seamless reduced basis element method for 2D Maxwell's problem: an introduction, in: Spectral and high order methods for partial differential equations, Vol. 76 of Lect. Notes Comput. Sci. Eng., Springer, Heidelberg, 2011, pp. 141–152.

[9] D. B. P. Huynh, D. J. Knezevic, A. T. Patera, A static condensation reduced basis element method: approximation and *a posteriori* error estimation, ESAIM Math. Model. Numer. Anal. 47 (1) (2013) 213–251.

[10] D. B. P. Huynh, D. J. Knezevic, A. T. Patera, A static condensation reduced basis element method: complex problems, Comput. Methods Appl. Mech. Engrg. 259 (2013) 197–216.

[11] K. Smetana, A new certification framework for the port reduced static condensation reduced basis element method, Comput. Methods Appl. Mech. Engrg. 283 (2015) 352–383.

[12] L. Iapichino, Reduced basis methods for the solution of parametrized PDEs in repetitive and complex networks with application to CFD, Ph.D. thesis, EPFL, Lausanne (2012).

[13] L. Iapichino, A. Quarteroni, G. Rozza, Reduced basis method and domain decomposition for elliptic problems in networks and complex parametrized geometries., Computers & Mathematics with Applications 71 (1) (2016) 408–430.

[14] I. Martini, G. Rozza, B. Haasdonk, Reduced basis approximation and a-posteriori error estimation for the coupled stokes-darcy system, Advances in Computational Mathematics (2014) 1–27.

[15] F. Albrecht, B. Haasdonk, S. Kaulmann, M. Ohlberger, The localized reduced basis multiscale method, in: Proceedings of contributed papers and posters, 2012, pp. 393–403.

[16] S. Kaulmann, M. Ohlberger, B. Haasdonk, A new local reduced basis discontinuous Galerkin approach for heterogeneous multiscale problems, C. R. Math. Acad. Sci. Paris 349 (23-24) (2011) 1233–1238.

[17] G. Rozza, K. Veroy, On the stability of the reduced basis method for Stokes equations in parametrized domains, Comput. Methods Appl. Mech. Engrg. 196 (7) (2007) 1244–1260.

[18] A. Quarteroni, G. Rozza, A. Manzoni, Certified reduced basis approximation for parametrized partial differential equations and applications, J. Math. Ind. 1 (2011) Art. 3, 44.

[19] C. Canuto, M. Y. Hussaini, A. Quarteroni, T. A. Zang, Spectral Methods. Evolution to Complex Geometries and Applications to Fluid Dynamics, Springer, Heidelberg, 2007.

[20] C. Canuto, M. Y. Hussaini, A. Quarteroni, T. A. Zang, Spectral Methods. Fundamentals in Single Domains, Springer, Heidelberg, 2006.
[21] A. Toselli, *hp* discontinuous Galerkin approximations for the Stokes problem, Math. Models Methods Appl. Sci. 12 (11) (2002) 1565–1597.
[22] P. Houston, D. Schötzau, T. P. Wihler, Energy norm a posteriori error estimation for mixed discontinuous Galerkin approximations of the Stokes problem, J. Sci. Comput. 22/23 (2005) 347–370.
[23] V. Girault, B. Rivière, M. F. Wheeler, A discontinuous Galerkin method with nonoverlapping domain decomposition for the Stokes and Navier-Stokes problems, Math. Comp. 74 (249) (2005) 53–84.
[24] B. Rivière, Discontinuous Galerkin methods for solving elliptic and parabolic equations, Vol. 35 of Frontiers in Applied Mathematics, Society for Industrial and Applied Mathematics, Philadelphia, PA, 2008.
[25] I. Mazzieri, Non-conforming high order methods for the elastodynamics equation, Ph.D. thesis, Politecnico di Milano (2012).
[26] Y. Bazilevs, T. J. R. Hughes, Weak imposition of Dirichlet boundary conditions in fluid mechanics, Comput. & Fluids 36 (1) (2007) 12–26.
[27] A. Quarteroni, Numerical Models for Differential Problems, 2nd ed., Springer, 2014.
[28] M. F. Wheeler, An elliptic collocation-finite element method with interior penalties, SIAM J. Numer. Anal. 15 (1) (1978) 152–161.
[29] D. N. Arnold, An interior penalty finite element method with discontinuous elements, SIAM J. Numer. Anal. 19 (4) (1982) 742–760.
[30] D. N. Arnold, F. Brezzi, B. Cockburn, L. D. Marini, Unified analysis of discontinuous Galerkin methods for elliptic problems, SIAM J. Numer. Anal. 39 (5) (2001/02) 1749–1779.
[31] C. Bernardi, Y. Maday., Approximations Spectrales de Problèmes aux Limites Elliptiques, Springer Verlag, Paris, 1992.
[32] J. M. Boland, R. A. Nicolaides, Stability of finite elements under divergence constraints, SIAM J. Numer. Anal. 20 (4) (1983) 722–731.
[33] A. Quarteroni, A. Valli, Domain decomposition methods for partial differential equations, Oxford University Press, 1999.
[34] G. Rozza, D. B. P. Huynh, A. Manzoni, Reduced basis approximation and a posteriori error estimation for Stokes flows in parametrized geometries: roles of the inf-sup stability constants, Numer. Math. 125 (1) (2013) 115–152.
[35] P. F. Antonietti, P. Gervasio, P. Pacciarini, A. Quarteroni, A unified discontinuous Galerkin Reduced Basis Element approach for the approximation of second order parametrized partial differential equations on partitioned domains, Tech. rep., in preparation (2016).
[36] F. Ballarin, A. Manzoni, A. Quarteroni, G. Rozza, Supremizer stabilization of POD-Galerkin approximation of parametrized steady incompressible Navier-Stokes equations, Int. J. Numer. Meth. Engrg. 102 (5) (2015) 1136–1161.